mation about the direction of the segment. Some models of imaginary small crystals comprising tens of chain segments that are set to make the three-dimensional lattice of orthorhombic PE were considered in the calculation. The (100) contact plane of PE whose chain axis orients in the [010] direction of $(CH_2)_{36}$ is the most probable. In the case of a normal paraffin ($C_{36}H_{74}$), the most stable orientation is obtained when a set of chain segments with the (110) contact plane orient in the ⟨110⟩ directions of $C_{36}H_{74}$ and the second most stable is the [010] orientation with a (110) contact plane. These stable contact planes are also predicted by lattice mismatching. The contact planes thus predicted are in good agreement with those observed in surface decoration of monoclinic cycloparaffins ($(CH_2)_{36}$ and $(CH_2)_{60}$) and orthorhombic normal paraffins ($C_{36}H_{74}$ and $C_{94}H_{190}$).[6,8,9]

Acknowledgment. This work was partly supported by a Grant-in-Aid for Scientific Research from the Ministry of Education, Science and Culture, Japan. K.J.I. gratefully acknowledges a fellowship from the Rotary Yoneyama Memorial Foundation, Inc.

References and Notes

(1) Fischer, E. W. *Kolloid Z. Z. Polym.* **1958**, *159*, 108.
(2) Hattori, Y.; Ashida, M.; Watanabe, T. *Nippon Kagaku Kaishi* **1975**, *3*, 496. Ueda, Y.; Ashida, M. *J. Electron Microsc.* **1980**, *29*, 38.
(3) Mauritz, K. A.; Baer, E.; Hopfinger, J. *J. Polym. Sci., Polym. Phys. Ed.* **1973**, *11*, 2185.
(4) See, for example: Organization of Macromolecules in the Condensed Phase. *Faraday Discuss. Chem. Soc.* **1979**, 68.
(5) Wittmann, J. C.; Lotz, B. *Makromol. Chem., Rapid Commun.* **1982**, *3*, 733.
(6) Wittmann, J. C.; Lotz, B. *J. Polym. Sci., Polym. Phys. Ed.* **1985**, *23*, 205.
(7) Georgiadis, T.; Manley, R. St. J. *J. Polym. Sci., Polym. Lett.* **1971**, *9*, 297.
(8) Ihn, K. J.; Tsuji, M.; Isoda, S.; Kawaguchi, A.; Katayama, K.; Tanaka, Y.; Sato, H. *Makromol. Chem., Rapid Commun.* **1989**, *10*, 185.
(9) Ihn, K. J.; Tsuji, M.; Isoda, S.; Kawaguchi, A.; Katayama, K.; Tanaka, Y.; Sato, H. *Macromolecules*, preceding paper in this issue.
(10) Mauritz, K. A.; Hopfinger, J. *J. Polym. Sci., Polym. Phys. Ed.* **1976**, *14*, 1813.
(11) Isoda, S. *Polymer*, **1984**, *25*, 615.
(12) Boistelle, R. *J. Cryst. Growth* **1978**, *43*, 141.
(13) Kitaigorodsky, A. I. *Organic Chemical Crystallography*; Consultant's Bureau: New York, 1955; 322.
(14) Bunn, C. W. *Trans. Faraday Soc.* **1939**, *35*, 482.
(15) Trzebiatowski, T.; Dräger, M.; Strobl, G. R. *Makromol. Chem.* **1982**, *183*, 731.
(16) Teare, P. W. *Acta Crystallogr.* **1959**, *12*, 294.
(17) Scott, A.; Scheraga, H. A. *J. Chem. Phys.* **1966**, *45*, 2091.
(18) Ihn, K. J.; Tsuji, M.; Isoda, S.; Kawaguchi, A.; Katayama, K.; Tanaka, Y.; Sato, H. *Makromol. Chem.* **1989**, *190*, 837.
(19) Kawaguchi, A.; Ohara, M.; Kobayashi, K. *J. Macromol. Sci., Phys.* **1979**, *B16*, 193.

Registry No. PE, 9002-88-4; $(CH_2)_{36}$, 297-50-7; $C_{36}H_{74}$, 630-06-8.

High-Temperature Structures of Poly(*p*-hydroxybenzoic acid)[1]

Do Y. Yoon,* Norberto Masciocchi,[2] Laura E. Depero,[3] Christopher Viney,[4] and William Parrish

IBM Almaden Research Center, 650 Harry Rd., San Jose, California 95120-6099.
Received June 20, 1989; Revised Manuscript Received September 1, 1989

ABSTRACT: The structures of poly(*p*-hydroxybenzoic acid) (PHBA) at the two high-temperature phase transitions (ca. 340 and 430 °C) have been investigated by X-ray powder diffraction methods (X-ray tube focusing and synchrotron parallel beam), chain conformation/packing models, and dielectric measurements. The structure of PHBA between ca. 340 and 430 °C, derived from the X-ray patterns and available electron diffraction results, is satisfactorily accounted for by the following model: orthorhombic cell, a = 9.24 Å, b = 5.28 Å, and c = 12.50 Å, with two successive phenylene planes along the c-axis rotated 60° from each other in the unit cell; the phenyl groups in the a–b plane are oriented in an ordered herringbone-type packing in each phenyl layer with their planes 60° and 120° with respect to the a-axis; and each chain segment (of two monomer repeats) in the unit cell is positioned randomly in the a–b projection among the two different sites involving a twofold axis of reorientation through an angle π. The dielectric constants at high frequencies (100 kHz) indicate rapid chain mobility accompanying this high-temperature phase. This structure of PHBA therefore follows quite well the model of the smectic-E phase of small rodlike molecules. The second transition around 430 °C involves no change in the packing order along the chain axis or chain conformations but only the loss of long-range phenyl orientation order in the a–b plane, very much like the smectic-E to smectic-B transition of small rodlike molecules. The coherence length along the chain axis of PHBA crystals at room temperature is estimated to be ca. 2700 Å, according to the Sherrer formula, and this packing order along the chain axis is maintained throughout the two high-temperature transitions. Relevance of the smectic-type high-temperature structures of PHBA to the molecular order in aromatic copolyesters comprising majority HBA monomers is then discussed.

Introduction

The structures of the homopolymer poly(*p*-hydroxybenzoic acid) (PHBA), $-(C_6H_4-C(=O)O-)_x$, at high temperatures have been the subject of a considerable number of investigations,[5–11] owing to their close connection to the nature of molecular order in thermotropic copolyesters of commercial interest.[8,12–15] These copolyesters

0024-9297/90/2223-1793$02.50/0

comprise mostly HBA groups (ca. 70%) plus one or two comonomer moieties to bring down the processing (flow) temperature to practical ranges, since the PHBA homopolymer is virtually unprocessible by normal methods.[5,7] These aromatic copolyesters with a majority of HBA moieties quite often exhibit X-ray patterns very much like those of PHBA homopolymer at high temperatures. Hence, studies of high-temperature structures of PHBA are very critical to understanding the structure–property relationships of a number of important aromatic copolyesters.

Recently, Economy et al.[7] showed that PHBA exhibits two phase transitions at ca. 340 and ca. 445 °C, respectively, on the basis of differential scanning calorimetry (DSC) and thermomechanical analyzer (TMA) measurements. They concluded that the first transition at 340 °C is either a crystal to a plastic crystal or to a high-order smectic phase transition and that the second transition at 445 °C results in a nematic phase.

The high-temperature structures of PHBA above 340 °C were studied separately by Blackwell et al.,[8] Lieser,[9] and Li et al.[10] by electron diffraction and by Hanna and Windle[11] by X-ray powder diffraction. The unit cell parameters showing an orthorhombic cell located in a hexagonal net ($a = 3^{1/2}b$) and two monomer repeats with 2_1 screw symmetry along the c-axis are thus well established. So far, all the diffraction results have been discussed only qualitatively in terms of three-dimensional crystals, possibly involving conformational disorder.[9,11] Hanna and Windle specifically pointed out the presence of three-dimensional order up to 450 °C,[11] thus disputing the conclusion of Economy et al.[7] that PHBA exhibits a nematic phase above ca. 445 °C. Hanna and Windle also reported continuous decrease in the crystalline peak intensities with increasing temperature above 350 °C and hence did not discuss the second transition.[11] Therefore, no satisfactory quantitative explanation of the experimental diffraction data has been presented from the molecular conformation/packing model for either of the two high-temperature phases of PHBA.

In this paper, we present first the detailed X-ray powder diffraction results of PHBA at room temperature and the structural changes occurring at the two high-temperature transitions. Our experimental results, which are much improved over the previously published data[5,11] as a consequence of minimizing the thermal degradation effects and improving the methods, demonstrate clearly the occurrence of the two transitions observed by Economy et al.[7] Comparison with model calculations leads to the detailed picture of the chain conformations and packing, which can be described by smectic-E and smectic-B types, respectively, both well-known for the small rodlike molecules.[16] Dielectric relaxation results at high frequencies are then presented which clarify the dynamic nature of the disorder consistent with the proposed smectic-type order. Finally, relevance of our findings to the structures of thermotropic copolyesters is discussed.

Experimental Section

PHBA Samples. The PHBA sample was obtained as powders from Polysciences, Inc. (cat. 4306). Its DSC diagram (Figure 1), obtained with Du Pont 910 DSC, indicates that the average degree of polymerization ($\overline{DP}$) is quite high, >100, upon comparison with the results of Economy et al. on the $\overline{DP}$ dependence of the first transition temperature.[7] For the X-ray measurements, the coarse particles were first removed by mechanical separation, and the remaining fine particles were then spread on a thin (0.4-mm) silicon single-crystal wafer surface, cut parallel to the 510 plane to minimize substrate scattering, by use of 5% collodion in amyl acetate as a binder. For the dielectric experiments, the PHBA powders were compression sintered at ca. 300 °C to form thin disks of ca. 1-mm thickness and 25 mm in diameter, and patterned aluminum electrodes were deposited subsequently by vacuum evaporation before carrying out the measurements with the HP 4275A LCR meter.

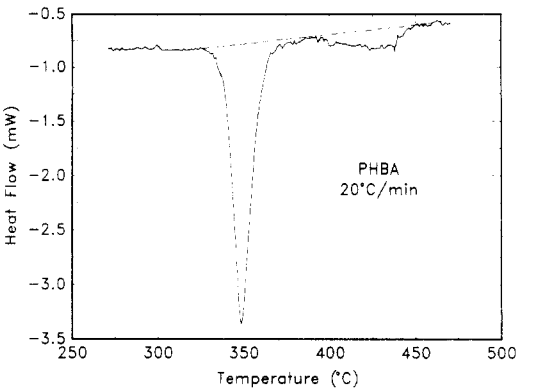

Figure 1. DSC trace of PHBA polymer as received at a heating rate of 20 °C/min. The dashed line denotes the approximate base line.

X-ray Measurements. The X-ray patterns were recorded by using a vertical-scanning-type powder diffractometer operating in a standard θ–2θ geometry.[17] The experimental parameters were as follows: copper target line focus X-ray tube operated at 50 kV/25 mA, 0.5° entrance slit to define the primary beam, antiscatter slits, a 0.12° (2θ) receiving slit, 4° Soller slit in the incident beam (only) to limit axial divergence, and a curved graphite monochromator placed after the receiving slit to reflect the Cu Kα radiation only. This geometry gives reflection profiles of 0.16° (2θ) full width at half-maximum (fwhm) when a silicon powder standard is used. The diffraction patterns were normally step-scanned from 10° to 50° (2θ) at the temperatures below 365 °C and from 10° to 36° (2θ) at higher temperatures. Separate overnight runs were performed at room temperature and 345 °C, ranging from 10 to 70° 2θ, with $\Delta 2\theta$ = 0.02°, t = 15 s, to obtain good counting statistical accuracy. A Na(Tl)I scintillation counter with pulse amplitude discrimination was used. Automated step-scan data recording and graphics display were done with an IBM PC/AT personal computer, allowing selection of the scan range, step increment, and count time. Recorded data were transferred to a host computer (IBM 3090) for analysis.

For the high-temperature X-ray measurements, the specimen was heated from below by clamping the thin silicon 510 plate to a flat silicon nitride plate containing an electric heating element.[19] A cylindrical heat shield with long beryllium window fit over the heater, and an outer vacuum-tight chamber with Mylar window covered the assembly. The temperature of the specimen was measured by a chromel–alumel thermocouple in contact with the silicon plate and maintained by a digital temperature controller (Omega CN5001K2). During the initial calibration, two external thermocouples were used to check the uniformity of the temperature distribution on the specimen area, which was found to be about 1% of the temperature setting. However, the X-ray phase changes were occurring at about 15–20 °C below the DSC value. This difference may have been caused by a small displacement of the thermocouple tip from the silicon wafer and/or the much faster heating rate of 20 °C/min used in DSC scans. It was decided to correct the X-ray temperature values reported in this paper by a linear correction factor based on the DSC data. The diffraction experiments were performed under low vacuum (0.5 Torr), in order to avoid air scatter and absorption losses and to prevent possible oxidation of the specimen.

Some higher resolution diffraction patterns were measured at room temperature with synchrotron radiation by using 1.5372-Å X-rays, close to the Cu Kα wavelength for the conventional X-ray tube studies. Each reflection is a single profile rather than the Kα doublet. The parallel beam method using a long parallel slit collimator gives narrow symmetrical profiles with

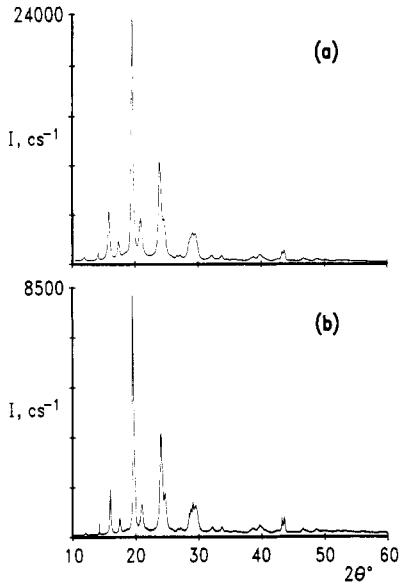

Figure 2. Room temperature X-ray diffraction powder data for PHBA (as received): (a) tube-focusing X-ray data; (b) parallel beam synchrotron data.

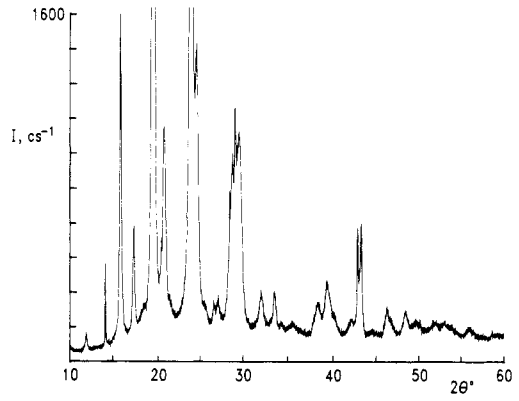

Figure 3. Enlarged plot of Figure 2b, high-resolution synchrotron pattern.

fwhm of 0.05° (2θ) and low background when using well-crystallized specimens. Although synchrotron radiation patterns generally have higher intensity than those observed with a conventional X-ray tube, the patterns in Figures 2 and 3 are lower because a smaller specimen was used, and the current of the storage ring was very low at the time this pattern was recorded. The specimen was continuously rotated at 65 rpm around the scattering vector to obtain better averaging of the particle distribution. One full pattern of PHBA was recorded with step-scanning of $\Delta 2\theta = 0.02°$ and count time 2 s, over the 2θ range 10–60°.

Data Analysis. Data reduction included calculation of linear background, peak identification, and 2θ determination by the cubic first derivative method.[20] The computer program was also used to calculate the full width at half-maximum (fwhm) for the separated peaks. Other programs were used to determine the unit cell parameters in a trial and error indexing procedure independent of any literature values,[21] to refine the unit cell parameters after proper indexing had been performed,[22] and to calculate the positions and indices of diffraction maxima corresponding to the given set of unit cell parameters.[23]

Results and Discussion

Room Temperature X-ray Results. The high-resolution data recorded at room temperature with synchrotron radiation compare well with the diffraction pattern obtained with standard focusing X-ray methods. They are shown in Figure 2, together with the expanded scale diagram of the synchrotron data in Figure 3. The patterns show that our PHBA sample was very highly ordered: the amorphous halo is nearly absent, and significant peaks are measurable up to 60° 2θ, with about 30 peaks clearly detected. The indexing of the major peaks according to the unit cell parameters of Geiss et al.[6] and phase I of Lieser,[9] determined from their electron diffraction measurements, approximately fits most of the observed data. The rhombohedral unit cell reported by Economy et al.[5] was discarded because no reasonable match was found with our peak positions.

Table I
Synchrotron X-ray Diffractometry Data for PHBA Crystals at Room Temperature

hkl	2θ(obs), deg	2θ(calc), deg	*d*(calc), Å	*I*(obs)[a]
100	11.89	11.81	7.47	1
002	14.08	14.07	6.28	3
110	19.57	19.59	4.52	100
111	20.81	20.84	4.25	11
200	23.93	23.74	3.74	42
004	28.40	28.35	3.14	7
113	28.98	29.01	3.07	12
211	29.43	29.41	3.03	11
203	31.99	32.02	2.79	2
120	33.52	33.72	2.65	2
006	43.09	43.11	2.09	5
304	46.43	46.40	1.95	1
400	48.61	48.59	1.87	1

[a] The observed intensities are the normalized peak heights after the background correction.

The unit cell parameters were then refined by using the 13 clearly indexable peaks belonging in phase I in the synchrotron experimental pattern (see Table I). The values were $a = 7.47$ Å, $b = 5.67$ Å, and $c = 12.55$ Å, orthorhombic system; the refined parameters obtained from the standard laboratory data were the same within 0.5 standard deviation. The unit cell volume, $V = 532$ Å^3, is consistent with four units of HBA per unit cell; the derived density is then $\rho_{calc} = 1.498$ g cm^{-3}, which is only slightly higher than the value reported by Geiss et al.[6] Although the *b* and *c* parameters agree with the electron diffraction data of Geiss et al.[6] and Lieser,[9] the observed *a* parameter is somewhat smaller than theirs (7.47 vs 7.62 (ref 6) and 7.52 Å (ref 9), respectively). Table I contains the indices, the observed and calculated peak positions, and the relative experimental peak intensities of the synchrotron data, after correction for primary beam intensity decay and background subtraction.

The unit cell parameters presented here are mainly for the purpose of comparing with those of high-temperature structures. A detailed analysis of the room temperature X-ray pattern by molecular modeling, including the presence of a small amount of phase II crystals,[9] will be discussed separately.[30]

The 00*l* reflections have the sharpest peaks in the pattern, indicating a quite large coherence length along the *c*-axis; this sharpness allows the resolution of 004 and 006 peaks from the overlapping clusters in the synchrotron pattern (Figure 3). For quantitative estimates, the width of the 002 peak in the tube-focusing X-ray pattern was corrected for the instrumental broadening and, assuming 100% Lorentzian shape, used subsequently to calculate the domain size *L* by use of the Scherrer formula fwhm $= k\lambda/L \cos\theta$.[25] Assuming $k = 0.9$,[24] $L(002)$ is estimated to be ca. 2700 Å, corresponding roughly to 220 unit cell repeats along the *c*-axis. For comparison, $L(200)$ is estimated to be ca. 240 Å, applying the same procedure.

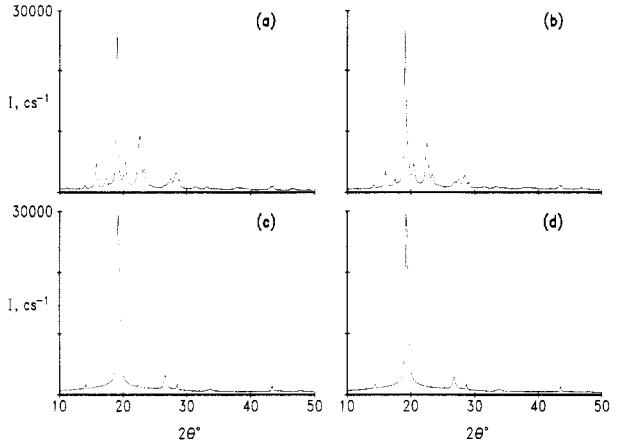

Figure 4. X-ray diffraction powder data for PHBA across the first phase transition: (a) 270, (b) 300, (c) 325, and (d) 345 °C.

Table II
Temperature Dependence of the Lattice Parameters and Unit Cell Volume (V) of PHBA

T, °C	a, Å	b, Å	c, Å	V, Å^3
25	7.47	5.67	12.55	531
270	7.79	5.68	12.52	554
300	7.78	5.67	12.53	554
325	9.23	5.26	12.51	607
335	9.23	5.27	12.50	608
345	9.24	5.28	12.50	610
355	9.26	5.29	12.50	612
365	9.27	5.30	12.49	614
390	9.27	5.35	12.49	619
410	9.31	5.36	12.47	622
430	9.35	5.40	12.46	629

High-Temperature X-ray Results. When the specimen is heated in the range 270–435 °C, the positions and relative intensities of most peaks change. Two phase transformations have been detected in the X-ray experiments that correspond to the DSC transitions. Figure 4 shows the patterns recorded across the first phase transition. At temperatures between 325 and 390 °C, all but one of the peaks (at approximately 26.6° 2θ) can be indexed on the basis of a hexagonal unit cell with dimensions of about 5.3 × 5.3 × 12.5 Å; the additional reflection can be indexed if we assume an orthorhombic unit cell with a = 9.24 Å, b = 5.28 Å, and c = 12.50 Å at 345 °C. Specifically, $a \simeq 3^{1/2}b$. Similar lattice parameters are reported by Blackwell et al.[8] on the basis of electron diffraction results. The small number of observed peaks is due to the relationship $a = 3^{1/2}b$ that leads to superposition of reflections $h_1k_1l_1$ and $h_2k_2l_2$ if $h_1^2 + 3k_1^2 = h_2^2 + 3k_2^2$. Examples of such pairs are 110 and 200, 020 and 310, and 116 and 206.

As at room temperature, the c repeat distance corresponds to the length of a dimeric unit, and the absence of 00l reflections with l odd suggests the continued presence of a 2_1 screw axis parallel to c. The change of the lattice parameters with increasing temperature, listed in Table II, shows a slight contraction in this chain repeat distance at higher temperatures, in agreement with the previous result.[11] The unit cell volume (which always contains four HBA units) is plotted against temperature in Figure 5, showing an abrupt increase of 9.5% accompanying the first transition.

After the sample was heated to a maximum temperature of 365 °C, the specimen was slowly cooled to 260 °C in about 4 h (the heating from room temperature to 365 °C took about the same time), and the reversibility of the observed phase transition was ascertained by performing measurements at several intermediate temperatures. Table III summarizes a few data for the 110, 002, and 004 reflections and their measured full widths at half-maximum (fwhm), as tracked during the heating run.

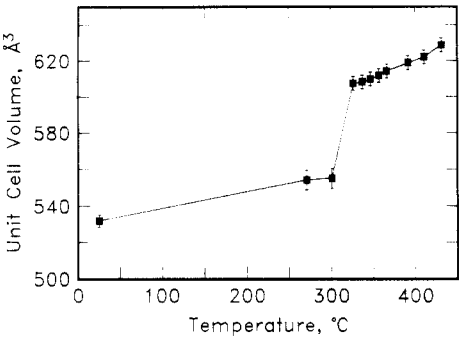

Figure 5. Temperature dependence of the unit cell volume; each unit cell contains four monomeric units.

Further heating of the sample to 435 °C showed the details of the second phase transition consistent with the small change in the measured enthalpy (see Figure 1): the only significant change in the X-ray pattern is the gradual disappearance of the peak at about 26.6° 2θ. Figure 6 shows the data recorded at 365, 390, 410, and 435 °C. At 435 °C, PHBA possesses the true hexagonal symmetry in the a–b plane, with the following refined parameters: a = 5.40 Å and c = 12.45 Å; only three peaks, 002, 100, and 004, were observed in the range 10–36° 2θ.

PHBA Structure above the First Transition near 340 °C. The data recorded during a separate overnight run at 345 °C with standard focusing geometry are shown in Figure 7a. The patterns are characterized by the very strong peak, labeled 110/200, the tiny but sharp peaks corresponding to the 00l sequence (l = 2 at 14.17° 2θ, l = 4 at 28.52°, l = 6 at 43.40°), and many more low-intensity peaks. The unit cell, as discussed above, is orthorhombic with a = 9.24 Å, b = 5.28 Å, and c = 12.50 Å. The relation $a = 3^{1/2}b$ implies that the molecules are indeed positioned on a hexagonal net when viewed in projection along c. Hence, one would obtain a true hexagonal symmetry in the a–b plane if the PHBA chains were considered to be cylindrical rods. However, as discussed previously, the strong peak at 26.64° 2θ can only be indexed within an orthorhombic symmetry. It follows then that the relative orientation of chain segments in the a–b plane cannot be described by a plastic crystal or a rotator-phase crystal that involves free (or random) rotations around the chain axis.

This situation is very similar to that of the smectic-E phase of small rodlike molecules, n-pentyl 4-((4′-phenylbenzylidene)amino)cinnamate (PPBAC), for example. The packing of aromatic phenylene groups in the smectic-E phase of PPBAC has been described as herringbone packing, as shown schematically in Figure 8.[16] In this typical herringbone packing, however, the 210 reflection appears as a strong intensity peak, since the adjacent 210 planes have an interlayer plane with a different phenyl orientation, as shown by the solid and dashed lines in Figure 8. The absence of a 210 reflection in Figure 7a therefore indicates that the two different planes in Figure 8 (solid and dashed) should be identical. This means that the successive phenyl planes along the chain axis are not coplanar but staggered. Furthermore, the presence of the strong 211 peak indicates that the phenyl staggering results in a stacking (along c) of identically oriented phenyl groups with a relative shift of $1/[2(a + b + c)]$. This relationship of phenyl packing symmetry is shown schematically in the left side of Figure 9, where the upper phenylene of the unit cell is denoted by the

Table III
Temperature Dependence of the Intensity[a] and Full Width at Half-Maximum (fwhm)[b] of Selected Peaks of PHBA

	002		110		004	
T, °C	*I*(peak)	fwhm	*I*(peak)	fwhm	*I*(peak)	fwhm
25	1950	0.21	69 500	0.31		
270	1800	0.24	84 400	0.27		
300	2050	0.25	81 300	0.27		
325	2550	0.23	87 100	0.44	2700	0.23
345	3050	0.23	87 900	0.44	3300	0.23
365	2600	0.23	87 100	0.44	2300	0.23
390	2700	0.23	83 900	0.40	2150	0.23
410	2900	0.23	88 500	0.34	1850	0.23
430	3450	0.23	78 200	0.37	2400	0.23

[a] *I*(peak) refers to the peak intensity after the background correction. [b] fwhm in degrees.

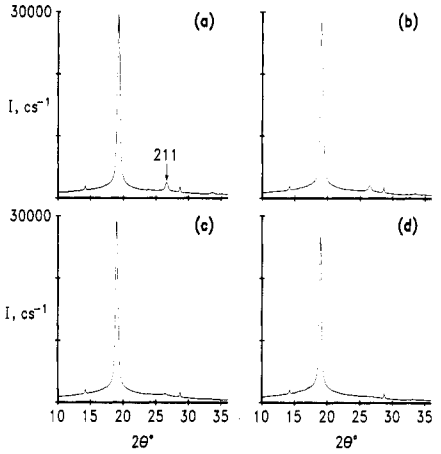

Figure 6. X-ray diffraction powder data for PHBA across the second phase transition: (a) 365, (b) 390, (c) 410, and (d) 435 °C.

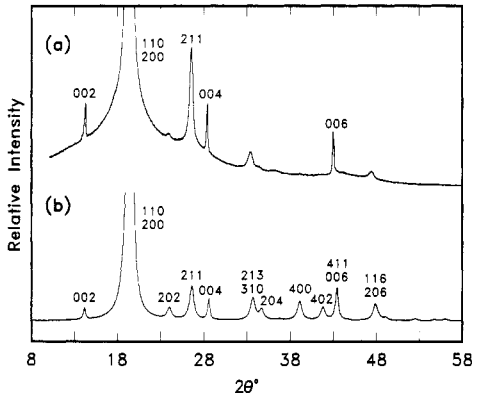

Figure 7. Comparison of experimental data at 345 °C (a) and the calculated pattern (b) computed from the structural model described in the text.

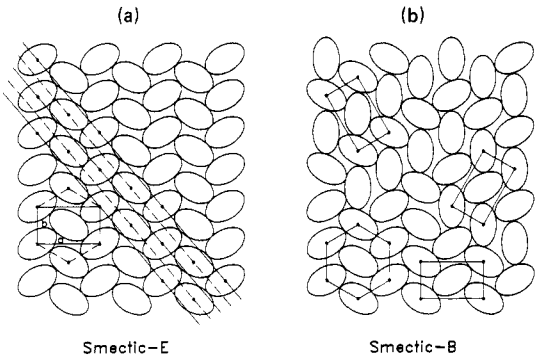

Figure 8. (a) Herringbone packing of phenylene rings in the *a*–*b* plane, corresponding to a smectic-E phase; the solid and dashed lines belong to two different sets of 210 planes with different orientation of the phenylene units. (b) Smectic-B packing showing the possibility of local hexagonal symmetry and three different orientations of orthorhombic subcells.

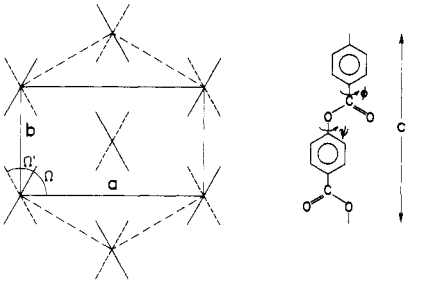

Figure 9. Orthorhombic unit cell for the smectic-E phase of PHBA, projected along and perpendicular to the *c*-axis, showing the chain conformation and the relative staggered orientation of the phenylene rings. In the left side, the solid lines denote the upper rings and the dashed lines denote the lower rings, respectively.

solid line and the lower one by the dashed line in the projection on the *a*–*b* plane.

However, in the detailed atomistic picture, the phenylene positions do not occur with their centers at the node of the lattice, as shown schematically in the right side of Figure 9. One example of this phenyl projection is shown in i and ii of Figure 10, where the torsional angles ϕ and ψ are 30° and −30°, respectively. The required phenyl packing symmetry then makes it necessary to introduce the disorder, as in the case of the smectic-E phase of small rodlike molecules,[16,25] involving a twofold axis of reorientation through an angle π for each (two-monomer) repeat unit around the *c*-axis. This is exemplified by the structure labeled i′ in Figure 10. The angle between the *a*-axis and the phenyl planes, Ω and Ω′ in Figure 9, could then be determined by comparing the calculated X-ray patterns with the experiments.

Model Calculations. The calculated X-ray powder patterns were obtained by using the method of Smith and Holomany[23] and employing the molecular geometries of PHBA tabulated by Hummel and Flory[26] from the crystal structures of model compounds. The disorder was accounted for by including all the resulting atomic positions in the computations. The appropriate space group is then described *Pba*2. A good fit was achieved by taking Ω = Ω′ = 60°, as shown in Figure 7b. Here, each peak is represented by a Lorenzian curve with the peak area corresponding to the calculated intensity, and the width (fwhm) was approximated to be 0.3° for the 00*l* and 0.6° for all the other peaks, respectively. The calculated relative intensities are also listed in Table IV.

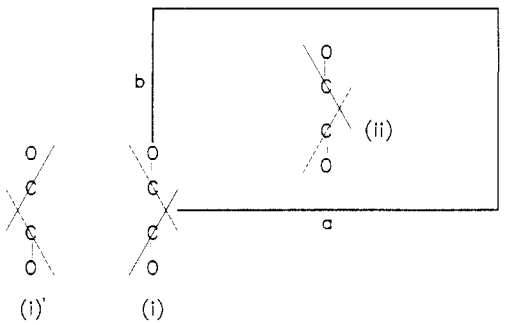

Figure 10. Actual location in the unit cell of the phenylene rings (solid and dashed lines) and the carbonyl units; solid lines denote the upper rings and the dashed ones the lower rings: (i) static situation along the 0,0,z axis; (ii) static situation along the $a/2,b/2,z$ axis; (i') effect of π reorientation of the PHBA chain segment i around the c-axis.

Table IV
Calculated X-ray Peak Intensities for PHBA at 345 °C

hkl	2θ, deg	relative intensities
002	14.2	1.5
200	19.3	100.0
110	19.3	36.4
202	24.0	2.8
211	26.6	8.6
004	28.5	2.7
213	33.5	1.2
310	33.7	4.6
204	34.7	2.5
400	39.1	4.8
402	41.8	3.2
411	43.4	2.7
006	43.4	2.8
206	47.9	3.1
116	47.9	1.0

The calculated intensities are in good agreement with experimental intensities except those of the 400 and 402 peaks. While the 400 peak is not noticeable in Figure 7a, this peak is clearly seen in the electron diffraction patterns of Blackwell et al.[8] and Li et al.[10] This difference between X-ray and electron diffraction results may reflect the fact that electron diffraction, due to its capability to isolate the PHBA particles with highest order, is not influenced by the presence of other less ordered particles. The absence of 400 and 402 peaks in the X-ray measurements, averaging over all the particles, then suggests that the most prevalent disorder is the small-scale lattice disorder along the a-axis. Furthermore, all the other peaks listed in Table IV are in good agreement with the electron diffraction experiments.[8,10] Of particular interest is the model prediction that the intensity of the 200 peak is substantially higher than that of the 110 peak. While this cannot be checked by X-ray patterns, the electron diffraction results[8] are in excellent agreement with this model prediction.

PHBA Structure above the Second Transition near 430 °C. The second transition near 430 °C, as shown by the DSC results of Economy et al.[7] and Figure 1, is marked by the disappearance of the 211 reflection in Figure 6. This is demonstrated also in Figure 11, which shows the intensity changes of various peaks as a function of temperature. We find that all the sharp peaks except 211 maintain their intensities up to 435 °C. Therefore, the rapid decrease of the 211 intensity at high temperatures is not due to the thermal degradation at all and hence should reflect the real phase transition. This transition is analogous to the smectic-E to smectic-B transition of small rodlike molecules,[16,27] involving the loss of long-range coherence of orthorombic lattice in the a–b plane

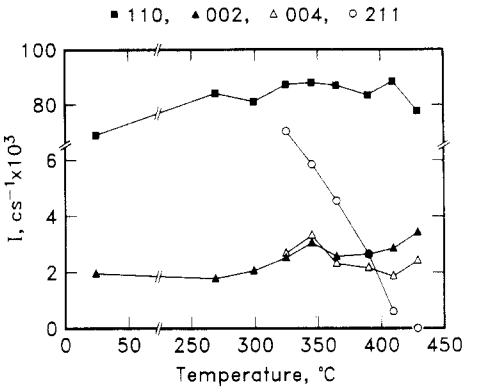

Figure 11. Peak intensity (after background subtraction) of the 002, 110, 211, and 004 reflections vs temperature.

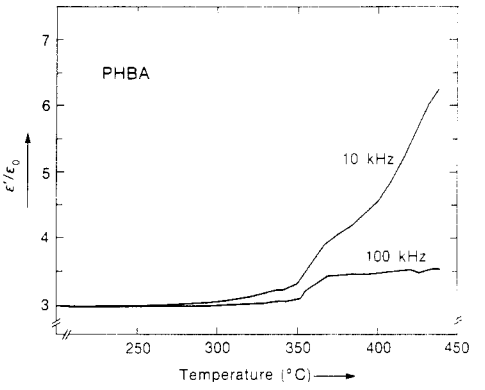

Figure 12. Dielectric permittivity ϵ' of PHBA vs temperature at 10 and 100 kHz, respectively. Measurements taken at every 2 °C interval are connected by lines. The experimental errors, not shown here, are due to the uncertainties in the sample dimensions and the void content that represent a constant multiplication factor for all temperatures and frequencies and hence do not affect the relative values.

while the herringbone packing on the hexagonal lattice is preserved locally, as shown schematically in Figure 8b. In the smectic-B phase, the local chain conformations and their twofold reorientational disorder are nearly identical with those of the smectic-E phase. Whether the same situation also holds for PHBA cannot be ascertained by the X-ray results since the freely rotating "rotator phase" or "plastic crystal" structure situated in the hexagonal lattice results in an identical X-ray diffraction pattern.

High-Temperature Dielectric Behavior of PHBA. The X-ray results alone cannot distinguish whether the twofold reorientational disorder in the smectic-E phase is static or dynamic in nature.[16,25] Moreover, X-ray results cannot discriminate between the smectic-B-type packing (Figure 8b) and the freely rotating plastic crystal packing. These questions have been addressed by dielectric, NMR, and incoherent neutron-scattering experiments in the case of small molecules. Here we report the results of dielectric results to clarify these questions for PHBA.

Figure 12 shows the dielectric permittivity ϵ' versus temperature at two frequencies of 10 and 100 kHz, respectively. Due to uncertainties in the sample dimension and possible void content, the absolute values of ϵ' are subject to some errors. But the relative values, most relevant for our purpose, are free of these uncertainties. At frequencies 10 kHz or lower, the dielectric permitivity shows a continuing increase with temperature due to conductivity effects. At 100 kHz, ϵ' shows a small step jump around 350 °C and then remains nearly constant up to ca. 440 °C. At this high frequency, therefore, the con-

ductivity effects become negligible. The step increment of $\Delta\epsilon'$ around 350 °C, corresponding to the appearance of the smectic-E phase, shows that the nature of the twofold reorientational disorder is dynamic, with rates exceeding 100 kHz.

The results in Figure 12 also indicate that the dielectric permitivity at 10 kHz, which reflects charge conductivity effects, shows an increase in slope around 350 and 410 °C, consistent with the increased softness of PHBA sample observed by the TMA experiments[7] around these temperatures. However, the value of ϵ' at 100 kHz shows no noticeable change between 370 and 440 °C. This indicates no appreciable change in chain conformations and the local disorder, consistent with the small amount of enthalpy change (Figure 1). This may be taken as a sign that the transition around 430 °C is very much like the smectic-E to smectic-B phase as drawn schematically in Figure 8, and hence it does not result in the freely rotating plastic crystal phase. This conclusion from the dielectric results is consistent with the recent ^{13}C NMR results.[28]

Summary

PHBA Results. We have investigated the structures of PHBA from room temperature up to ca. 435 °C by X-ray diffractometry, molecular model calculations, and dielectric relaxation measurements. At room temperature, the synchrotron measurements allow a more precise determination of peak positions and bring out the striking sharpness of all the 00l peaks. The estimated coherence length $L(002)$ is quite large, ca. 2700 Å according to the Sherrer formula. At high temperatures, the X-ray results demonstrate the occurrence of two phase transitions, in agreement with the previous finding of Economy et al.[7] from their DSC and TMA results. The nature of these transitions has been determined by fitting the experimental X-ray patterns with the calculated patterns based on conformation/packing models, in conjunction with the analysis of the high-frequency dielectric behavior. The order after the first transition around 340 °C is very much like the smectic-E phase of small rodlike molecules in that the phenyl groups are packed (in each phenyl layer) in the herringbone-type manner and exhibit a twofold dynamic reorientational disorder through an angle π around the chain (c) axis. The polymeric chain nature, however, places the successive phenyl planes along the chain staggered by ca. 60° instead of the coplanar arrangement. The second transition is analogous to the smectic-E to smectic-B transition, which involves no change in packing along the chain axis and chain conformation but only the loss of long-range orthorombic coherence in the phenyl packing. The packing order along the chain undergoes little change up to 435 °C, which is the maximum temperature that can be reached without significant thermal degradation, and no nematic or freely rotating plastic crystal phase is found up to this temperature.

Relevance to Aromatic Copolymers. The molecular order in aromatic copolyesters rich in HBA monomer content often causes these copolyesters to exhibit X-ray patterns very close to those of the high-temperature structures of PHBA.[8,12-15] but with broader peak widths. They have often been described as crystalline, and the X-ray peak intensities have been related to the degree of crystallinity. Quite often the degree of crystallinity thus determined is much larger than one would normally derive for the random copolymers,[12-15] thus creating considerable confusion. In view of our finding on PHBA, this confusion could be avoided if one regards this order in random copolyesters to be not crystalline but a mesophase, i.e., high-order smectic type, which is able to accommodate considerable disorder in the chemical repeat. The fact that these copolyesters exhibit considerable reorientational mobilities even in the highly ordered state[14,29] is entirely consistent with the smectic-type order as discussed above.

Acknowledgment. We thank IBM Italy for granting visiting scientist fellowships to N.M. and L.D. and also thank IBM U.K. for a visiting scientist fellowship awarded to C.V. We thank E. Hadziioannou for obtaining the DSC results, Dr. P. Destruel for the dielectric measurements, and Drs. J. Economy and J. Lyerla for stimulating this work.

References and Notes

(1) This work was presented in part in the American Physical Society meeting in New Orleans, March, 1988: Yoon, D. Y.; Depero, L. E.; Viney, C.; Parrish, W. *Bull. Am. Phys. Soc.* **1988**, *33* (3), 638.
(2) IBM World Trade visiting scientist. Permanent address: Istituto di Chimica Strutturistica Inorganica, Universitá di Milano, via Venezian 21, I-20133 Milano, Italy.
(3) IBM World Trade visiting scientist. Current address: Dipartimento di Ingegneria Meccanica, Universitá di Brescia, via Valotti 9, I-25060 Brescia, Italy.
(4) IBM World Trade visiting scientist. Current address: Department of Materials Science and Engineering, FB-10, University of Washington, Seattle, WA, 98195.
(5) Economy, J.; Storm, R. S.; Matkovich, V. I.; Cottis, S. G.; Nowak, B. E. *J. Polym. Sci., Polym. Chem.* **1976**, *14*, 2207.
(6) Geiss, R.; Volksen, W.; Tsay, J.; Economy, J. *J. Polym. Sci. Lett.* **1984**, *22*, 433.
(7) Economy, J.; Volksen, W.; Viney, C.; Geiss, R.; Siemens, R.; Karis, T. *Macromolecules* **1988**, *21*, 2777.
(8) Blackwell, J.; Lieser, G.; Guttierez, G. A. *Macromolecules* **1983**, *16*, 1418.
(9) Lieser, G. *J. Polym. Sci., Polym. Phys.* **1983**, *21*, 1611.
(10) Li, L. S.; Lieser, G.; Rosenau-Eichin, R.; Fischer, E. W. *Makromol. Chem., Rapid Commun.* **1987**, *8*, 159.
(11) Hanna, S.; Windle, A. H. *Polym. Commun.* **1988**, *29*, 236.
(12) Blackwell, J.; Biswas, A.; Gutierrez, G. A.; Chivers, R. A. *Faraday Discuss. Chem. Soc.* **1985**, *79*, 73. Biswas, A.; Blackwell, J. *Macromolecules* **1988**, *21*, 3158.
(13) Windle, A. H.; Viney, C.; Golombok, R.; Donald, A. M.; Mitchell, G. R. *Faraday Discuss. Chem. Soc.* **1985**, *79*, 55.
(14) Bechtolt, H.; Wendorff, J. H.; Zimmermann, H. J. *Makromol. Chem.* **1987**, *188*, 651.
(15) Field, N. D.; Baldwin, R.; Layton, R.; Frayer, P.; Scardiglia, F. *Macromolecules* **1988**, *21*, 2155.
(16) Doucet, J. In *The Molecular Physics of Liquid Crystals*; Luckhurst, G. R., Gray, G. W., Eds.; Academic Press: London, 1979; Chapter 14 and references therein.
(17) Parrish, W. *X-Ray Analysis Papers*; Centrex: Eindhoven, 1965.
(18) Parrish, W. *Aust. J. Phys.* **1988**, *41*, 101.
(19) Parrish, W.; Erickson, C. G.; Masciocchi, N., in preparation.
(20) Huang, T. C.; Parrish, W. *Adv. X-Ray Anal.* **1984**, *27*, 45.
(21) Werner, P. E. *TREOR-4, Trial and Error program for unknown powder patterns, version 4*; Department of Structural Chemistry, Arrhenius Laboratory, University of Stockholm, S 10691 Stockholm, Sweden, 1984.
(22) Benoit, P. H. *A Microcomputer package for indexing and least-squares refinement of powder diffraction data (Microcomputer version 3.0)*; Williams Hall 31, Geology, Lehigh University, Bethelem, PA, 18015, 1987.
(23) Smith, D. K.; Holomany, M. *A FORTRAN IV program for calculating x-ray powder diffraction patterns—Version 7*; College of Earth and Mineral Sciences, Department of Geosciences, The Pennsylvania State University, 1980.
(24) Scherrer, P. *Nachr. Göttinger Gesell.* **1918**, 98.
(25) Leadbetter, A. J.; Richardson, R. M.; Carlile, C. J. *J. Phys. (Les Ulis, Fr.)* **1976**, *37*, C3-65.
(26) Hummel, J.; Flory, P. J. *Macromolecules* **1980**, *13*, 479.
(27) Levelut, A. M.; Doucet, J.; Lambert, M. *J. Phys. (Les Ulis, Fr.)* **1974**, *35*, 773.
(28) Lyerla, J., private communication.
(29) Alhaj-Mohammed, M. H.; Davies, G. R.; Abdul Jawad, S.; Ward, I. M. *J. Polym. Sci. Polym. Phys.* **1988**, *26*, 1751.
(30) Iannelli, P., in preparation.

Registry No. HBA (homopolymer), 30729-36-3; HBA (SRU), 26099-71-8.